Al-Nahrain Journal for Engineering Sciences (NJES) Vol.20 No.1, 2017 pp.235 - 249

Thermal Performance Enhancement of Phase Change Materials (PCMs) by Using Metal Foams

Ihsan Y. Hussain
Mechanical Eng. Dep.
College of Engineering
University of Baghdad
drihsan@uobaghdad.edu.iq

Marwah Abdulkareem Jasim
Mechanical Eng. Dep.
College of Engineering
University of Baghdad

Abstract

An investigation of thermal conductivity enhancement, melting and solidification processes of Phase Change Materials (PCMs) by using metal foams has been carried out. Two models have been used in the experiments, model I for measuring the effective thermal conductivity of metal foam embedded in paraffin wax, and model II used as a small scale thermal energy storage device with and without metal foam for investigating melting and solidification processes of the PCM under different cooling conditions (natural and forced convection). The theoretical investigation involves analytical solution of two models, the semi-infinite medium for calculating the thermal conductivity, and the thermal energy storage system TESS has been analyzed including several assumptions for determining the convective heat transfer coefficient and the factors that controlling forced convection and solidification of the PCM. The experimental results show that the thermal conductivity of wax with 10 PPI metal foam increased by (37-39) times that of pure wax. Effects of pore density (10 and 40 PPI), metal foam, and mass flow rate on solidification process have been studied and the effects of pore density and metal foam on the melting process have also been investigated. The present experimental results have been compared with the available previous studies and gave a good agreement.

Key Words: Phase Change Materials, Metal Foam, Porosity, Pore Density (PPI).

Introduction

Phase change materials (PCMs), which release or absorb thermal energy during melting and solidification processes, are believed to have outstanding capability to store a massive amount of heat efficiently during their phase change processes. PCMs have been investigated in building application, industrial waste heat recovery, solar collectors, solar power plants, high-efficient compact heat sinks, solar cookers, and solar stills. Most PCMs suffer from the common problem of low thermal conductivities, being around 0.2 W/(m.K) for most paraffin waxes. This prolongs the charging and discharging period of TES systems. Therefore, a heat enhancement technology in PCMs is needed. Metal foams, which have high strength-to-density ratio, ultra light porous structure and relatively high thermal conductivity, are believed to be a promising material for enhancing heat transfer performance and reducing the charging and discharging periods of PCMs. Most of the studies adapted numerical methods of solution to the governing equations of the heat transfer through metal foams using phase change materials (PCMs). **Lafdi et al. [1]** studied experimentally the phase change material (PCM) infiltrated in a high thermal conductivity foam. An experimental setup had been built for measuring the temperature profiles and capturing the melting evolution of the phase change material (PCM) inside aluminum foams. The steady-state temperature of higher porosity aluminum foam was attained faster than that of aluminum foam with lower porosity. Also, the steady state temperature for the bigger pore size foam was reached faster than that of aluminum foam with smaller pore size foam. **Zhong et al. [2]** studied experimentally the phase change material (PCM) embedded in metal foam. The metal foam that used in the study was mesophase pitch based graphite foams (GFs) with a different thermal properties and pore-size. They used foams to increase the thermal diffusivity of PCM for latent heat TESS application. The thermal diffusivity of the Paraffin and GF composite was enhanced to 190, 270, 500, and 570 times to that of pure paraffin wax. **Zhao et al. [3]** experimentally investigated melting and solidification processes for the solid/liquid phase change. The phase change material that used in the study was paraffin wax RT58. The results indicated that the influence of metal foam was very significant on the heat transfer of solid/liquid phase change, particularly at the solid zone of phase change materials (PCMs). Even so, the addition of metal foam enhanced the overall heat transfer rate by 3–10 times. **Vadwala [4]** investigated a method of enhancing thermal conductivity of paraffin wax by making use of high porosity open cell metal foams experimentally. By adding metal foam, thermal conductivity of PCMs was shown to

increase by 16-18 times that of pure paraffin wax. **Tian and Zhao [5]** investigated the effects of metal foams on the heat transfer performance in phase change materials (PCMs). The numerical investigation was based on the two-equation non-equilibrium heat transfer model; the coupled heat conduction and natural convection were considered at liquid zones and phase transition. The numerical results were validated by experimental data. **Li et al. [6]** studied experimentally and numerically the heat transfer of paraffin wax embedded in open-celled metallic foams. The influence of foam morphology parameters on the wall temperature and the temperature uniformity inside the metal foam were investigated, including porosity and pore density. The high thermal conductivity of the foam matrix could enhance the melting heat transfer, though its existence suppresses the local natural convection. A numerical model considering the non-Darcy effect, thermal non-equilibrium, and local natural convection was proposed. The velocity, evolution of the solid-liquid interface location, and temperature field at various times were predicted. ***In the present work***, an investigation of thermal conductivity enhancement, melting and solidification processes of Phase Change Materials (PCMs) by using metal foams has been carried out.

Experimental Work

An experimental rig has been constructed in the Heat Transfer Lab, at the Mechanical Engineering Department, University of Baghdad were the experiments carried out, see figure (1). The wind tunnel has a calming section of length 900mm, test section made from Pyrex material with dimensions (300 mm x 150 mm) and 294 mm length, calming section of length 682 mm, conical section with length 874 mm, inlet diameter 300 mm and outlet diameter 200 mm, the fan, driven by a single phase (AEI) A.C. motor with a speed of 2850 rpm, and valve by which the flow rate of air can be controlled through opening gate from 0 % to 100 %, the mean velocity at the test section used in the present work is (2.23, 3.16, 4.08, 5.77 and 6.7 m/s) at (20%, 40%, 60%, 80% and 100%) valve openings, respectively. The pore Reynolds number based on these velocities for (10PPI) are (125.1, 176.9, 228.4, 323, and 375.3), see table (1) and for (40PPI) are (78.6, 111.1, 143.4, 202.8, and 235.7), see table (2) respectively. Some measurements have been conducted on the copper foams samples of (10PPI & 40PPI) such as; porosity (ε), density, examination the purity of the copper foams, and examination of the number of pores per inch (PPI). Paraffin wax RT58 has been used as a phase change material (melting temperature range (44.2-51.9 °C), thermal conductivity 0.21 W/m.K, heat storage capacity 181 kJ/kg. Also, some measurements have been conducted on the paraffin wax such as; melting point, thermal conductivity, and density. Two models were used to perform the experiments as follows;

Model I

The experimental apparatus of model I consists of a rectangular copper foam with pore density of 10 PPI and 90% porosity. It was cut using band saw to the dimensions (300×20×20 mm) (L×W×H), a pure copper plate of (20×20 mm) (L×W) was placed in the bottom of the model in contact with the copper foam for better thermal contact and improves the thermal resistance, see figure (2). A 2 mm diameter holes were drilled on one face of the model at distances of 1, 2, 3, 5, 7, 9, 11 and 26 mm from one end of the model. Eight thermocouples (type-K)with a 0.25 mm diameter junction were inserted through the holes drilled in the model to measure the temperature variation along the length of the foam. The holes were then covered with an adhesive material resistant to high temperature to prevent leakage of wax. To ensure a leak-proof joint between copper plate and the model, rubber gasket and an adhesive material were applied on the mating surfaces of copper plate and the model. The adhesive material was allowed to dry for 24 hours. An electric heater is attached to the copper plate to melt the wax during the charging process.

Model II

A schematic drawing of the experimental setup is shown in figure (3). A rectangular copper foam with pore density of 10 and 40 PPI and 90% porosity has been cut to the dimensions (200×100×20) mm (L×W×H) embedded in paraffin wax RT58. The metal foams has been sintered with a copper plate of (100×200) mm in dimensions, an electric heater (200×100) mm in dimension (approximately same size as the test sample) used for melting the wax during the charging process and attached on the bottom surface of the copper plate to provide the continuous uniform heat flux. A 4 mm diameter hole is drilled on the middle of the plex cover. Two thermocouples (type-K) with a 0.25 mm diameter junction are inserted through the hole drilled in the model to measure the temperature variation. The holes are then covered with an adhesive material resistant to high temperature to prevent leakage of wax. To ensure a leak-proof joint between copper plate and the model, rubber gasket and an adhesive material were applied on the mating surfaces of copper plate and the model. The adhesive material was allowed to dry for 24 hours.

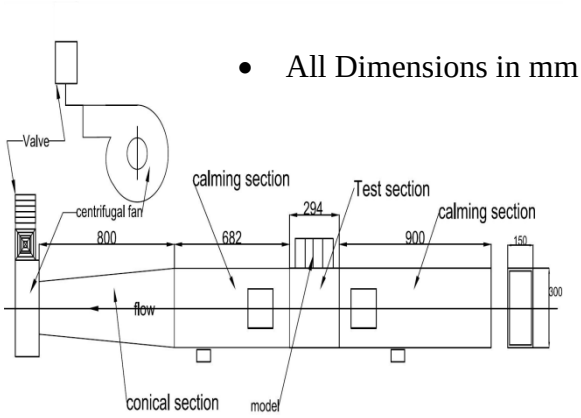

- All Dimensions in mm

Figure 1: Diagram of Experimental Apparatus

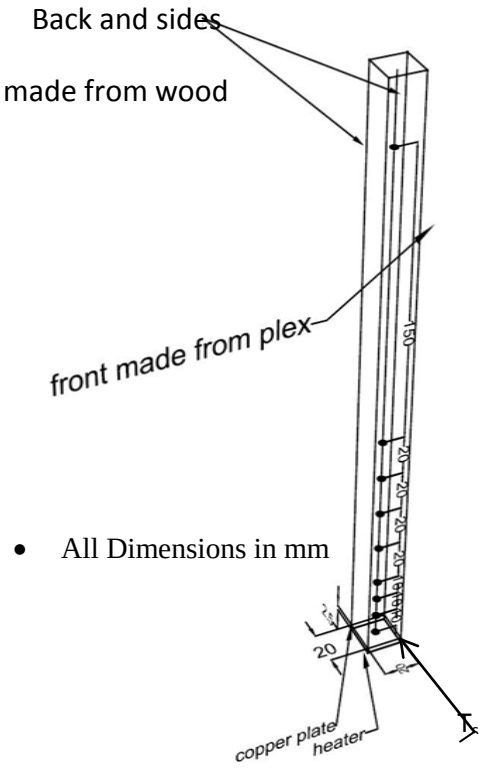

- All Dimensions in mm

Figure 2: Model I Geometry (all dimensions are in mm)

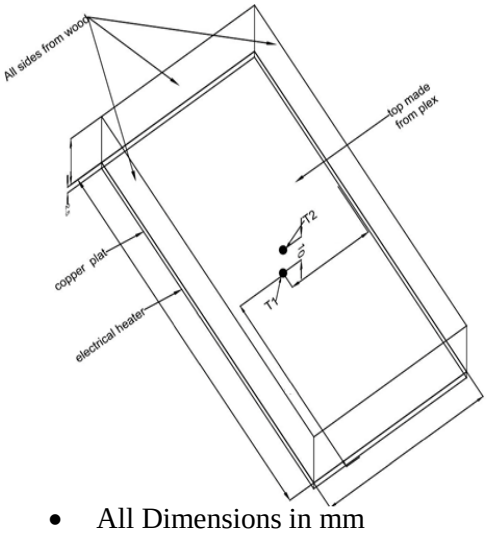

- All Dimensions in mm

Figure 3: Model II Geometry (all dimensions are in mm)

Table 1: Properties of Copper Foams (10PPI)

Parameters	Values
Porosity (ε)	0.90302
Permeability (K)	4.279×10^{-7} (m^2)
Friction Coefficient (C_f)	0.1665178
Forchheimer Form Drag Coefficient (C)	254.56 (m^{-1})
Density (ρ)	8663 (kg/m^3)
Thermal Conductivity (k)	401(W /m.C)
Specific Heat Capacity (C_p)	385 (J/kg .C)
Average pore Diameter (D_p)	905.7 µm

Table 2: Properties of Copper Foams (40PPI)

Parameters	Values
Porosity (ε)	0.8981
Permeability (K)	1.28355×10^{-7} (m^2)
Friction Coefficient (C_f)	0.16989
Forchheimer Form Drag Coefficient (C)	474.2 (m^{-1})
Density (ρ)	9095 (kg/m^3)
Thermal Conductivity (k)	401(W /m.C)
Specific Heat Capacity (C_p)	385 (J/kg .C)
Average pore Diameter (D_p)	568.6 μm

Data Processing

Metal foam embedded in paraffin wax is analyzed using the standard solutions used in analysis of heat conduction in semi-infinite medium described by **(Cengel 2007)**. Semi-infinite means that when a step change in temperature occurs at one end (x = 0) of a medium doesn't change the temperature at the other end (x = l) throughout the observation time. The temperature distribution along the length of the model for a constant surface temperature boundary condition (T_s = constant) is given by:

$$\frac{T(x,t)-T_i}{T_s-T_i}=\text{erfc}\left(\frac{x}{2\sqrt{\alpha t}}\right) \quad \dots (1)$$

where T(x,t): is the transient temperature measured at distance (x) from one end of the model and time (t), T_i: is the ambient (initial) temperature of the model, T_s: is the surface temperature which is held constant with the use of a temperature controller. By careful design of the model the constant surface temperature will be guaranteed since the surface area is too small (20 × 20 mm) compared to the length of the model (300 mm)m so there is no temperature variation. Thermal diffusivity (α) is the only unknown in equation (1) so it can be computed directly. To calculate the effective thermal conductivity the following relation is used:

$$k=\alpha.\rho_{eff}. \quad \dots (2)$$

These effective values are calculated by accounting for the volume fraction of each substance, based on porosity the resulting relation for effective density and effective specific heat are given as:

$$\rho_{eff}=\varepsilon.\rho_f+(1-\varepsilon).\rho_s \quad \dots (3)$$

$$c_{peff}=\varepsilon.c_{pf}+(1-\varepsilon).\ c_{ps} \quad \dots (4)$$

Where ε: is the porosity of copper foam and its value for (10 and 40 PPI) is (0.90). The subscripts f and s are used for fluid and solid phases respectively. The subscript eff denotes the effective value of a property.

In the present study, a theoretical three-dimensionally structured model developed by **Boomsma [9]** has been used to deal with the effective thermal conductivity of metal foam based on idealizing its structure as being a series of cells with the shape of a tetrakaidecahedron, see figure (4).

The developed equations of the model used to calculate the effective thermal conductivity are:

$$d=\sqrt{\frac{\sqrt{2}\left(2-\left(\frac{5}{8}\right)e^3\sqrt{2}-2\varepsilon\right)}{\pi(3-4e\sqrt{2}-e)}} \quad \dots (5)$$

$$R_A=\frac{4d}{\left(2e^2+\pi d(1-e)\right)k_s+\left(4-2e^2-\pi d(1-e)\right)k_f} \quad \dots (6)$$

$$R_B=\frac{(e-2d)^2}{(e-2d)e^2k_s+(2e-4d-(e-2d)e^2)k_f} \quad \dots (7)$$

$$R_C=\frac{(\sqrt{2}-2e)^2}{2\pi d^2(1-2e\sqrt{2})k_s+2\left(\sqrt{2}-2e-\pi d^2(1-2e\sqrt{2})\right)k_f} \quad \dots (8)$$

$$R_D=\frac{2e}{e^2k_s+(4-e^2)k_f} \quad \dots (9)$$

$$k_{eff}=\frac{\sqrt{2}}{2(R_A+R_B+R_C+R_D)} \quad \dots (10)$$

Where;

e: is the dimensionless cubic node length, its value was mentioned by the authors that it is a constant value equal to (0.339).

k_s: is the theoretical thermal conductivity of the copper foam (solid phase) which is equal to (400 W/mK).

k_f: is the theoretical thermal conductivity of paraffin wax (fluid phase) which is equal to (0.21 W/mK). k_{eff}: is the effective thermal conductivity of the composite system.

A detailed derivation of these equations is described by **Boomsma [9]**.

Model II

During the discharge process, the model was placed on the wind tunnel so that the bottom surface of the model (copper plate) had been exposed to forced air convection to cool it. Two thermocouples were placed in the wind tunnel one before the test section to measure air inlet temperature (T_{inlet}) and one after the test section to measure air outlet temperature(T_{outlet}), see figure (5).

To analyze the characteristics of the heat transfer of the TESS (thermal energy storage system), standard heat exchanger correlations is used described by **Cengel [7]**.

Physical properties of the fluid are evaluated at bulk mean temperature and 1 atm pressure

$$T_f=\frac{T_{inlet}+T_{outlet}}{2} \quad \dots (11)$$

The rate of convection heat transfer is described by Newton's law of cooling as:

$$Q=h_aA(T_s-T_f) \quad \dots (12)$$

From the energy balance, the heat transfer to the fluid (air) which flows through the wind tunnel is equal to the increase in energy of the fluid؛

$$Q=\dot{m}c_p(T_{f,outlet}-T_{f,inlet}) = h_aA(T_s-T_f) \quad \dots (13)$$

The value of convective heat transfer coefficient h_a is calculated by using equation (12), where T_s: is the copper plate temperature. Dimensionless numbers are defined using the concept of similitude which gives a means to compare systems with variable dimensions and flow parameters. In the laminar flow, the hydrodynamic entry length described by **Kays and Crawford [10]** is approximately:

$$L_{h,laminar}=0.05.Re.D_h \quad \dots (14)$$

The factors controlling forced convection are defined as:

Nusselt number:

$$Nu=\frac{h_aL_c}{k_f} \quad \dots (15)$$

Reynolds number

$$Re=\frac{\rho uL_c}{\mu} \quad \dots (16)$$

Where the mass flow rate ṁ is determined from;

$$\dot{m}=\rho uA_c \quad \dots (17)$$

Hydrodynamic Entry Length

The hydrodynamic entry length for Thermal Energy Storage System (TESS) was found by the equation (14), where the hydraulic diameter (D_h) of the wind tunnel test section (see figure (6.A)) is equal to:

$$D_h=\frac{2.a.b}{a+b} \quad (18)$$

Boundary layer thickness inside the Thermal Energy Storage System (TESS) (see figure (6.B)) is found from **Streeter 1987 [11]**:

$$\delta\approx\frac{5.x}{\sqrt{Re}} \quad \dots (19)$$

Type of the flow can be known by comparing the boundary layer thickness (δ) from equation (19) and the hydraulic entry length from equation (14). It was concluded that the flow was an external flow and the characteristic length was taken to be length of the copper plate (L_c =a).

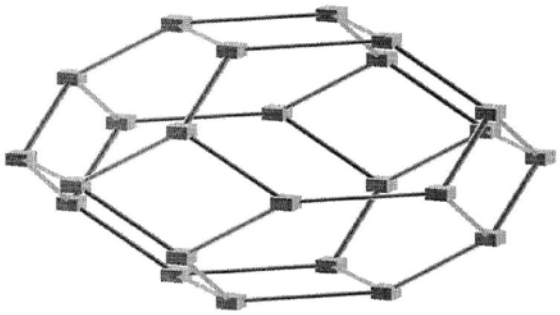

Figure 4 : A unit cell structure of tetrakaidecahedron with six squares and eight hexagons Boomsma [9]

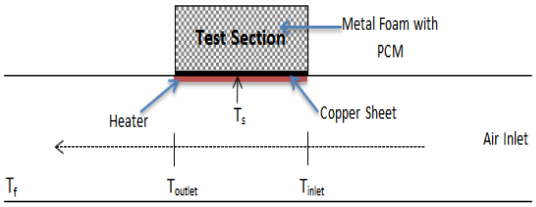

Figure 5: Model II Placed at the Top of the Wind Tunnel

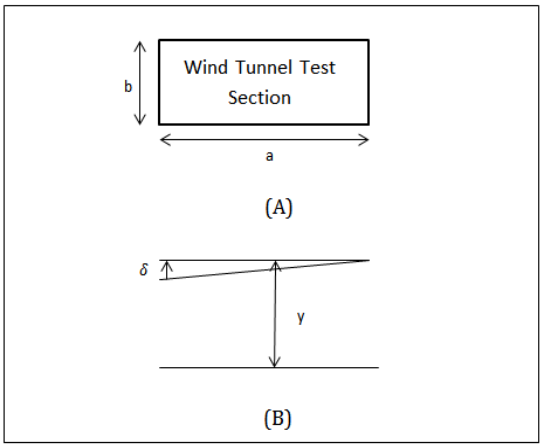

Figure 6: Thickness of Boundary Layer inside the Thermal Energy Storage System

Results and Discussions

Experimental Results:

In the experimental part of the present work, a total of 22 test runs have been carried out to cover all the possible investigated parameters.

To calculate thermal conductivity of metal foam impregnated with PCMs the test sample is treated as a semi – infinite medium. To prove that this was a reasonable assumption in these experiments, time varying temperatures at different points along the length of the model are plotted in Figure (7). From figure (7) one can be noticed that the temperature at a distance of x = 26 cm does not change even after 1500 seconds. Hence, the assumption that the model is semi – infinite medium is valid during the mentioned time interval. Figure (8) shows the values of

thermal diffusivity calculated from equation (1) for different temperatures and location. The figure shows that the thermal diffusivity value is initially higher and after about 560 seconds it reaches a constant value. At steady state the thermal diffusivity value starts dropping cause at steady state T(x,t) is a constant value and that leads to that the temperature terms on left hand side of equation (1) are all constant. From this, at steady state, thermal diffusivity is inversely proportional to time and as time is always increasing thermal diffusivity value starts dropping once steady state is reached, to neglect the initial and end effects and for simplicity, from figure (8) only the values that are within the two bounds are taken into account and then the average of these values was substituted into equation (2). The effective thermal conductivity is then calculated by substituting the values of thermal diffusivity and effective density and specific heat values into Equation (2). By substituting the values of thermal diffusivity and effective density and specific heat into equation (2), the effective thermal conductivity is then calculated. And its value come out to be (8.192 W/mK), compared to the theoretical value of (11.24 W/m.K), the percentage deviation is calculated from;

Percentage difference = $\frac{k_{eff_{theoretical}} - k_{eff_{experimental}}}{k_{eff_{theoretical}}} = 27.117\%$ … (20)

Solidification Process

In the present work, various parameters effect on the solidification process:

Effect of Pore Density (PPI)

Figure (9) shows the effect of pore densities (10 and 40 PPI) with a fixed porosity 0.9 at 80% air opening. It can be seen from the figure that the temperature gradient of foam wax-system with 10 PPI metal foam is greater than that of 40 PPI metal foam sample so metal foam sample with 40 PPI has better heat transfer performance than the one with 10 PPI. This is a reasonable result cause larger pore density means larger percentage of metal skeleton (larger contact area), which leads to enhance the heat transfer between the heating plate and air, also it can be seen from the figure that with 10 PPI metal foam paraffin wax takes around 1000 seconds to solidify whereas it takes around 700 seconds to solidify when 40 PPI metal foam was used. The time required to solidify the same amount of paraffin wax is reduced by 25% by using 40 PPI metal foam.

Effect of Metal Foam

The experimental results show that the effective thermal conductivity of the system with the use of 10 PPI metal foam is (37-39) times higher than that of pure wax, due to the addition of high porosity copper foam which provides a large solid-to-fluid surface area, and a high thermal conducting metallic phase, such as copper, which allow for enhanced heat transfer, so figure (10) shows that the foam-wax system solidifies more uniformly than the pure wax system, also it can be seen from the figure that at 80% air opening pure paraffin wax takes around 1300 seconds to completely solidify and paraffin wax with 10 PPI metal foam takes around 1000 seconds to solidify whereas it takes around 700 seconds to solidify when 40 PPI metal foam was used. The time required to solidify the same amount of paraffin wax is reduced by 23% by using 10 PPI metal foam and it is reduced by 46.2% with the use of 40 PPI metal foam.

Effect of Metal Foam on the Outlet Temperature of Air

Figure (11) discusses the effect of metal foam on the outlet temperature of air, it can be seen from the figure that with 10 PPI metal foam there was a small increase in the air outlet temperature (<2˚C) than that of paraffin wax only which helped to increase heat transfer during melting, but not during solidification. Also, figure (12) shows the inlet and outlet temperatures of air with time for 40 PPI metal foams.

Effect of Mass Flow Rate

Figure (13) shows the net effect of mass flow rate, the solidification time at 20% opening with 10 PPI metal foam was around 1900 seconds while at 100% opening it was around 800 seconds, so the solidification time is reduced by 57.9% when the air mass flow rate was higher at 100% air opening. Also the figure shows that the temperature distribution between the surface (T_1) and the center of the thermal energy storage system (TESS) (T_2) was higher at 100% opening.

Effect of Heat Transfer Mode

In the present work the model is subjected to two types of convection, forced and natural convection in the solidification process. Figures (14), (15) and (16) show solidification by natural convection with and without metal foams. With 10 PPI metal foam solidification time took around 4500 seconds and it took 4050 seconds with the use of 40 PPI metal foam while without metal foam it took around 5900 seconds. Figure (17) shows a comparison between forced and natural convection for foam-wax system with 10 PPI metal foam. The solidification time with natural convection takes 4530 seconds and it takes 1050 seconds with forced convection at maximum flow rate (100% air opening). The solidification time was reduced by 76.8% by using forced convection heat transfer. Nusselt number as a function of Reynolds number is plotted for wax with metal

foam (10 and 40 PPI) and for pure wax in figure (18), Nusselt number was calculated from equation (15) and Reynolds number was calculated from equations (16). It can be seen that adding copper foam (10 and 40 PPI) leads to an increase in the air outlet temperature and that resulted in much higher Nusselt number for the same Reynolds number. Nusselt number varies linearly with Reynolds number for all the cases, such that:

$Nu=0.399Re - 5966.2$ (for 40 PPI metal foam) … (21)

$Nu=0.4492Re - 7151.6$ (for 10 PPI metal foam) … (22)

$Nu=0.4146Re - 7318.5$ (for wax only) … (23)

Figure (19) shows the average convective heat transfer coefficient h_a ($W/m^2.K$) for different air openings. It can be seen from the figure that the convective heat transfer coefficient with the use of metal foam is higher than that pure PCM sample, and h_a varies linearly with the flow rate of air for all of the three cases;

$h_a=13777Q - 917.35$ (for 40 PPI metal foam) ... (24)

$h_a=14730Q - 954.31$ (for 10 PPI metal foam ... (25)

$h_a=13615Q - 972.44$ (for wax only) … (26)

Melting Process

Wax melts in the temperature range of (44.2-51.9), so it is considered that the melting process completed when T_2 reaches 70 ˚C. Figure (20) shows the temperature plotted as a function of time while melting for all the three cases (10 and 40 PPI) metal foam and without metal foam. It can be seen from figure (20.A) that the phase change of wax, with 40 PPI metal foam, starts at 300 second and ends at 930 second and figure (20.B) shows that with 10 PPI metal foam, the phase change of paraffin wax starts at 300 second and ends at 1080 second, while it can be seen from figure (20.C) that the phase change of wax, without metal foam, starts at 690 second and ends at 1140 second. For the effect of pore density (PPI).

Effect of PPI

Figure (21) shows that the total melting duration time were almost the same for different pore per inch (10 and 40 PPI), that was an acceptable result because at fixed porosity (0.9) volume fraction of the PCMs were identical. Also, it can be seen from the figure that paraffin wax with 40 PPI metal foam takes 1100 seconds to melt completely while it takes 1200 seconds with 10 PPI metal foam to completely melt, so the total melting duration time decreased by (8.3%) when 40 PPI metal foam was used.

Effect of Metal Foam

Figure (22) shows the effect of metal foam on the melting process, pure paraffin wax takes around 2250 seconds to completely melt while it takes around 1200 seconds to melt with the use of 10 PPI metal foam. The total melting duration time required for melting approximately the same amount of paraffin wax is reduced by (46.7%) when 10 PPI metal foams was used and with the use of 40 PPI metal foam it takes around 1100 seconds to melt completely. Also, the temperature gradient in paraffin wax with the use of metal foam is significantly lower than that without metal foam. By adding metal foam the effective thermal conductivity increased which leads to that reduction in temperature gradient, with the use of metal foam the temperature distribution is more uniform than it is in wax without metal foam. Figure (23.A) shows that when the slope of the temperature profile starts decreasing indicated that the phase change of paraffin wax (with 40 PPI metal foam) begins and it ends when the slope of temperature profile starts increasing again. From the figure, and by drawing tangents to the curve, it can be seen that phase change begins around 42˚C and it ends around 60˚C. Also it can be seen from the figure that the temperatures of phase change materials (PCMs) increase more slowly after melting begins, because the heat provided is mainly used for phase change rather than increasing sensible heat. After the state of phase change materials (PCMs) has become fully liquid (when temperatures are higher than 59 ˚C), its temperatures begin to increase more rapidly again, because the heat provided is now all used for increasing sensible heat of the PCMs, and it can be seen from figure (23.B) that the phase change of wax, with 10 PPI metal foam, starts around 42˚C and it ends around 59˚C.

Photographic Observation of Melting of the PCM

The propagation of wax without metal foam was photographed by a high speed camera 1000 fps (Casio/exilim 12.5 x), see figure (24). The photographs were taken 1140 seconds after the heater was turned one (after the beginning of the phase change). It can be seen from the photographed that the phase change ends after around 420 seconds from the begging of the photographing.

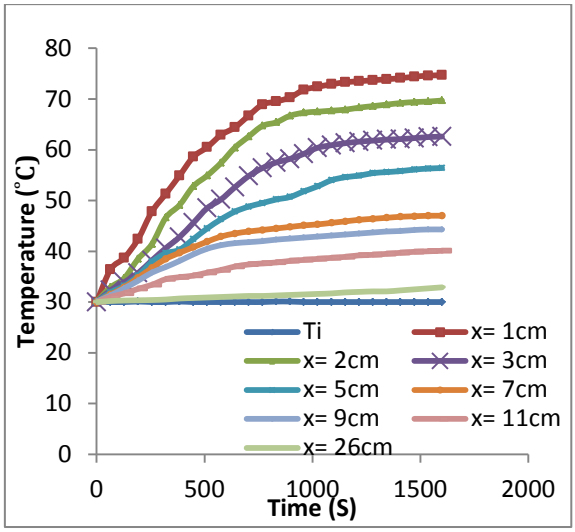

Figure 7: Experimental Obtained Temperature Results for T_s= 85 ˚C Plotted as a Function of time at Different Axial Distance along the Length of the Test Sample

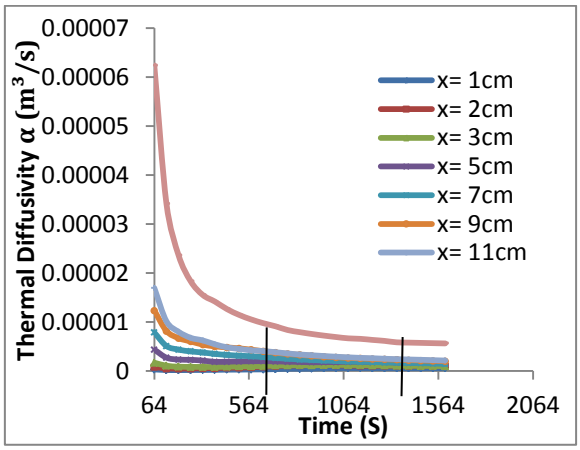

Figure 8: Calculated Thermal Diffusivity Values from Equation (1) at Different Distance along the Length of the Test Sample

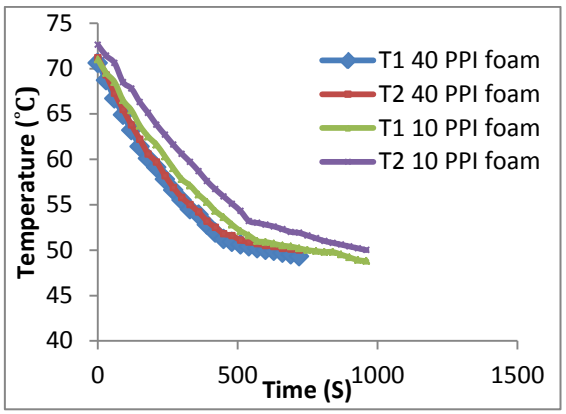

Figure 9: Experimentally Obtained Results of Different Pore Per Inch (10 and 40 PPI) Metal Foams at 80% Opening

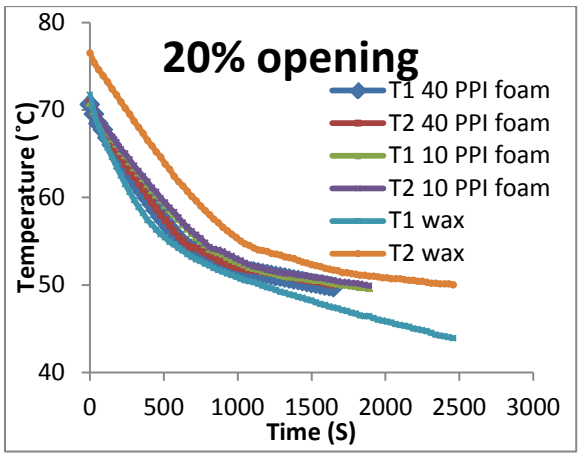

(A)

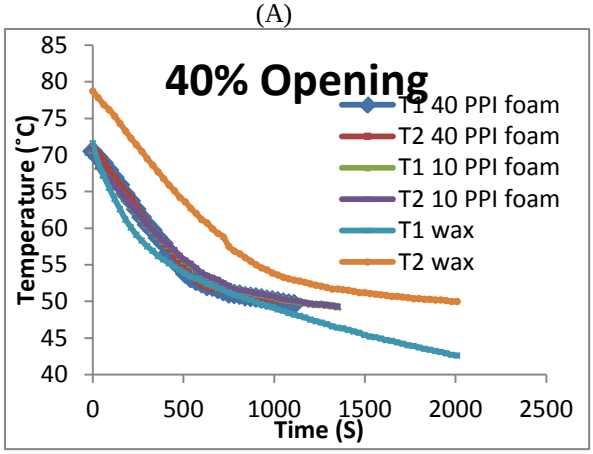

(B)

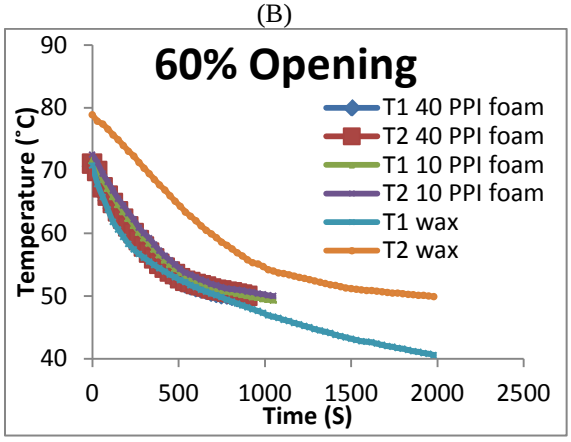

(C)

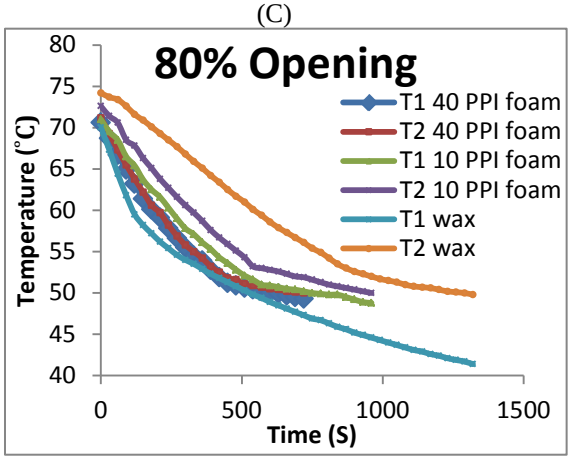

(D)

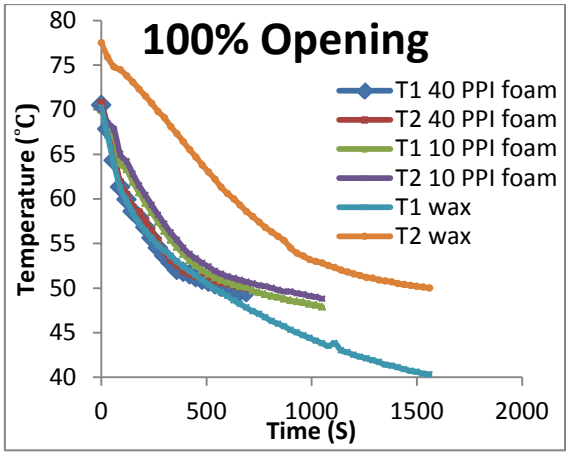

(E)

Figure 10 : Temperature History while Forced Solidification with Foam (10 and 40 PPI) and without Foam for Different Air Openings

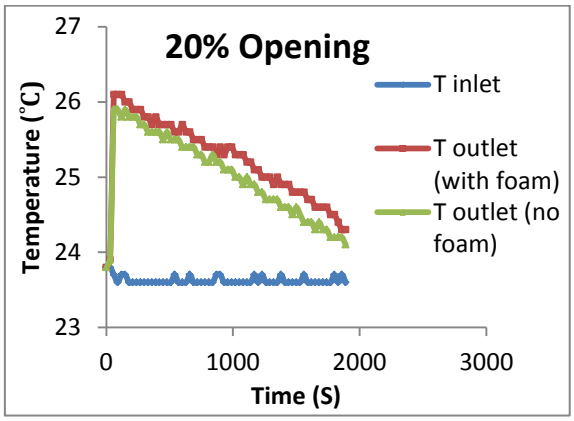

(A)

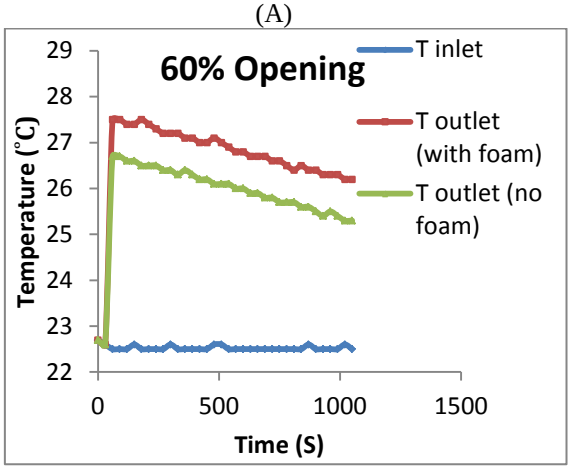

(B)

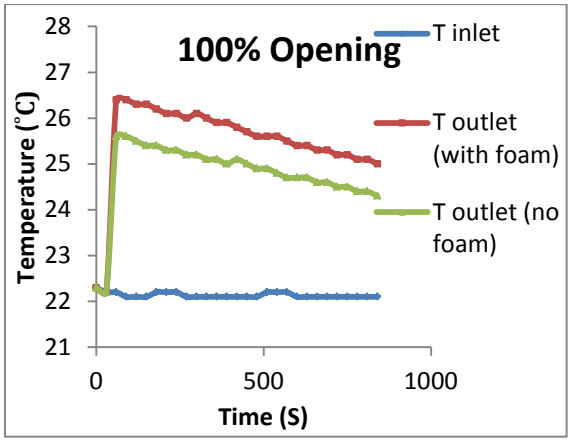

(C)

Figure 11: Variation of Inlet and Outlet Temperature of Air with Time for with and without Foam for Different Openings

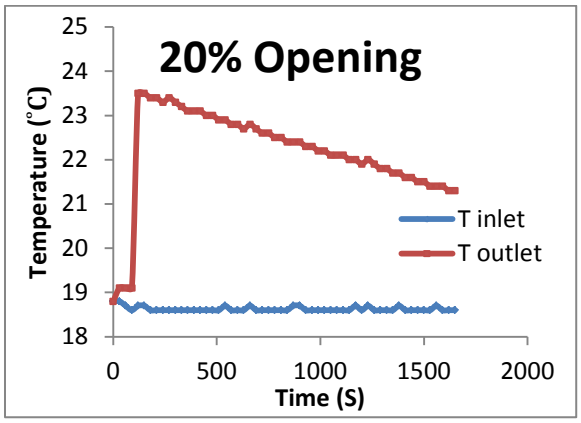

(A)

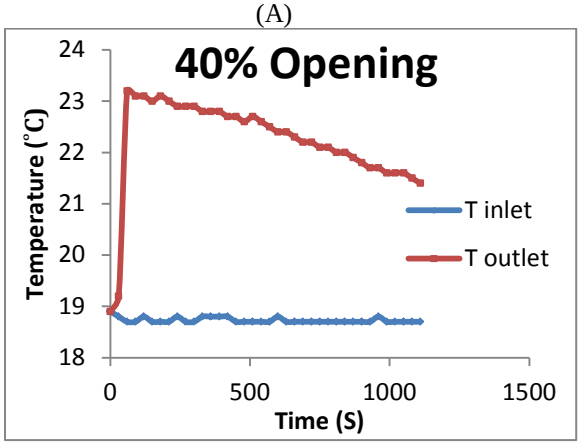

(B)

Figure 12 : Variation of Inlet and Outlet Temperature of Air with Time for 40 PPI metal foam

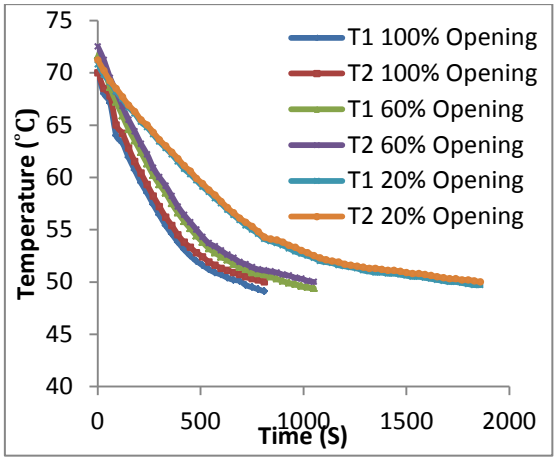

Figure 13: Solidification Process of Wax with 10 PPI Metal Foam for Different Air Openings

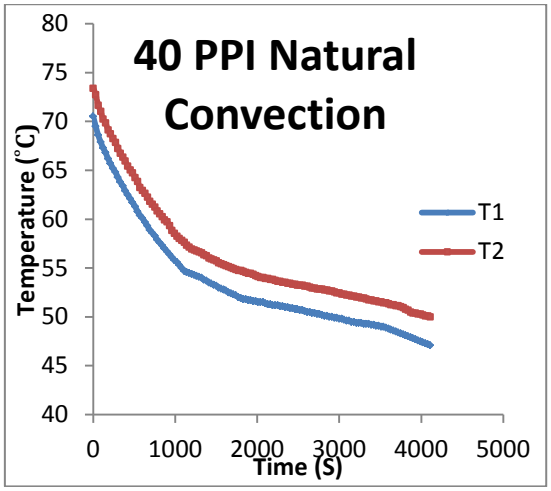

Figure 14 : Natural Convection Heat Transfer with 40 PPI Metal Foams

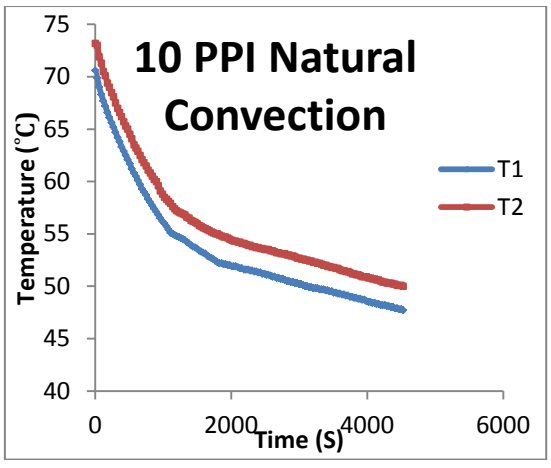

Figure 15 : Natural Convection Heat Transfer with 10 PPI Metal Foams

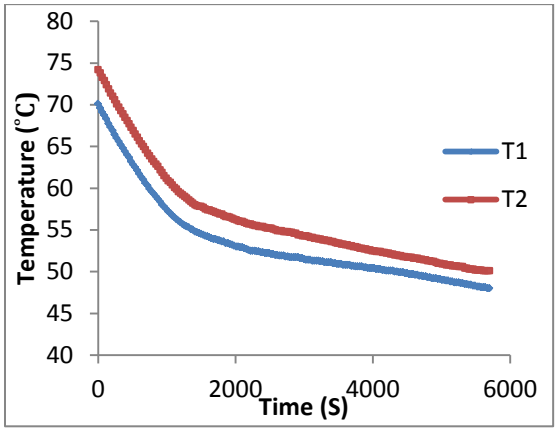

Figure 16 : Natural Convection Heat Transfer without Metal Foams

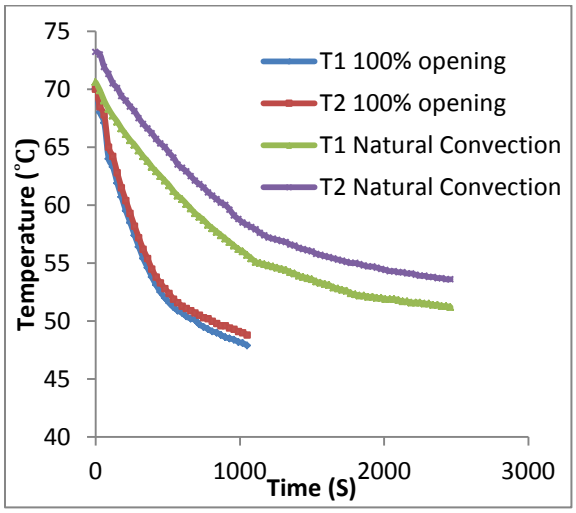

Figure 17: Comparison between Forced and Natural Convection

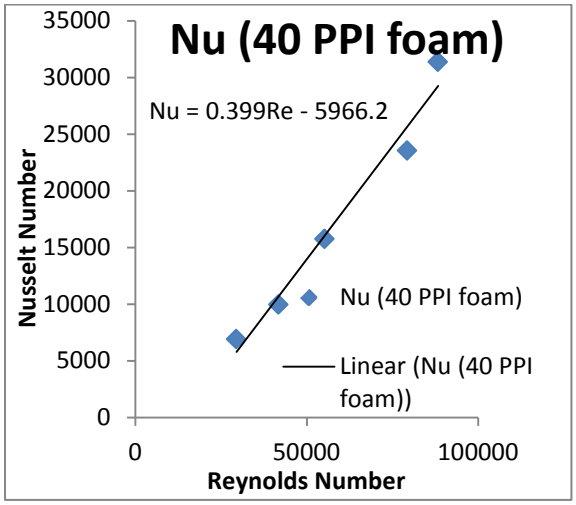

(A)

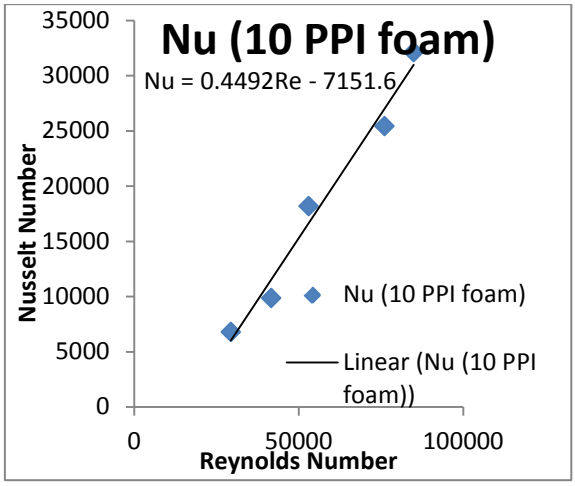

(B)

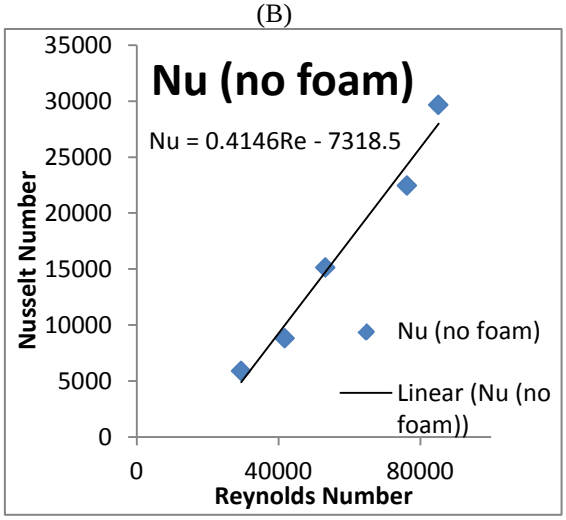

(C)

Figure 18: Nusselt Number with Respect to Reynolds Number for all Three Cases

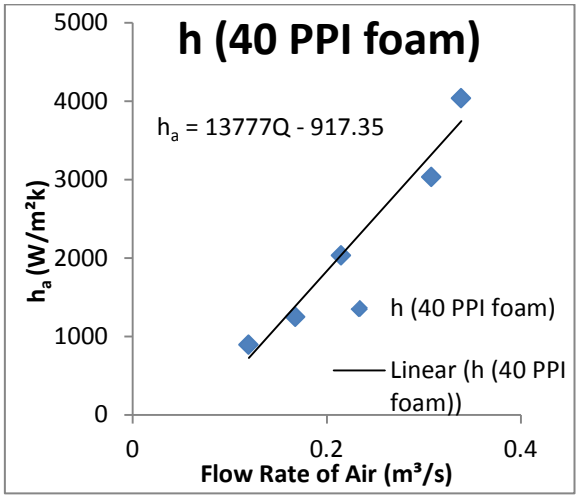

(A)

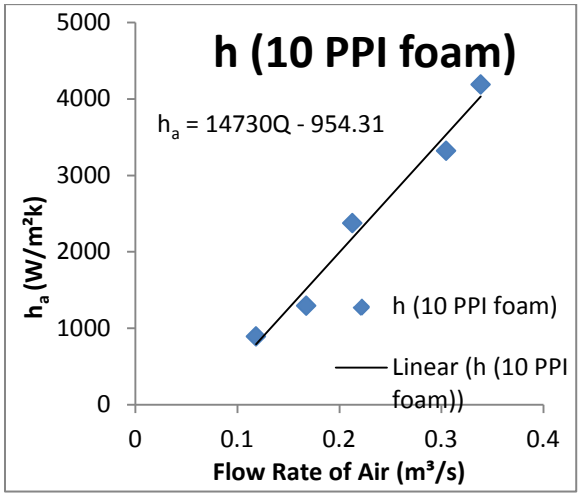

(B)

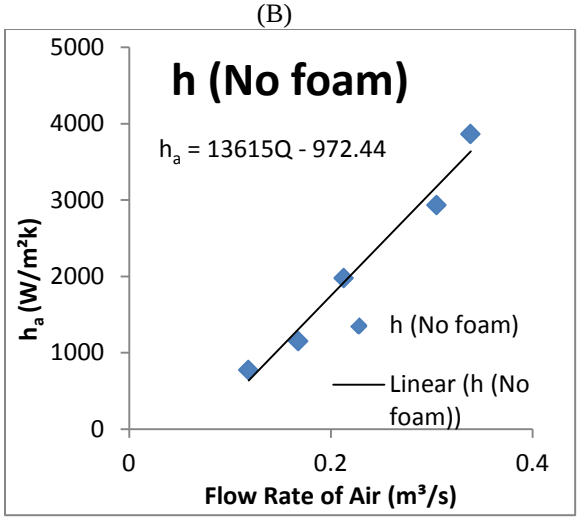

(C)

Figure 19 : Convective Heat Transfer Coefficient with Respect to Flow Rate of Air for all Three Cases

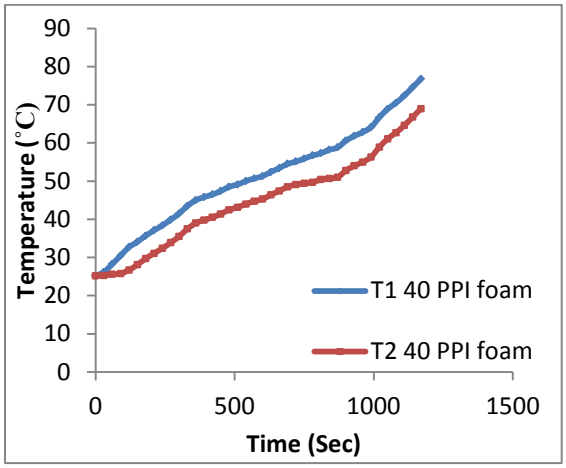

(A)

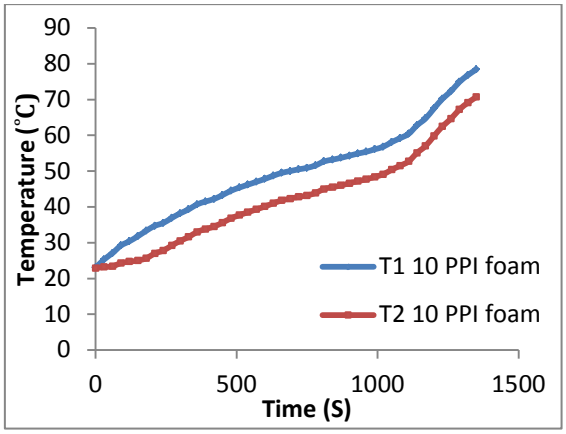

(B)

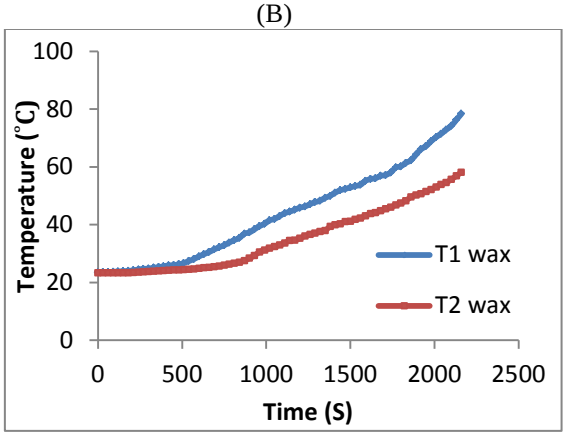

(C)

Figure 20 : Melting Process for All Three Cases

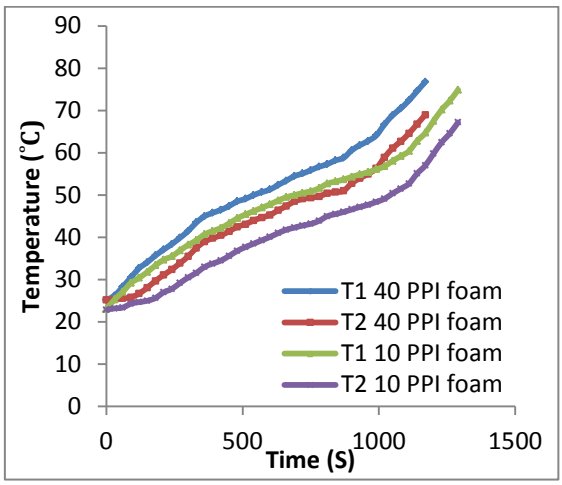

Figure 21: Melting Process of Paraffin Wax with (10 and 40 PPI) Metal Foams

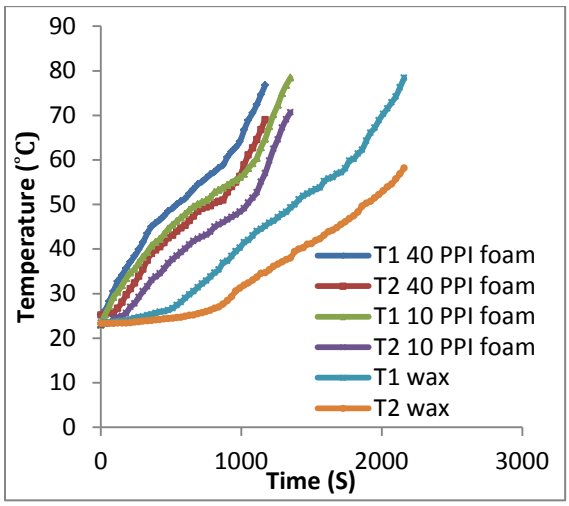

Figure 22: Melting Process of Paraffin Wax for all Three Cases

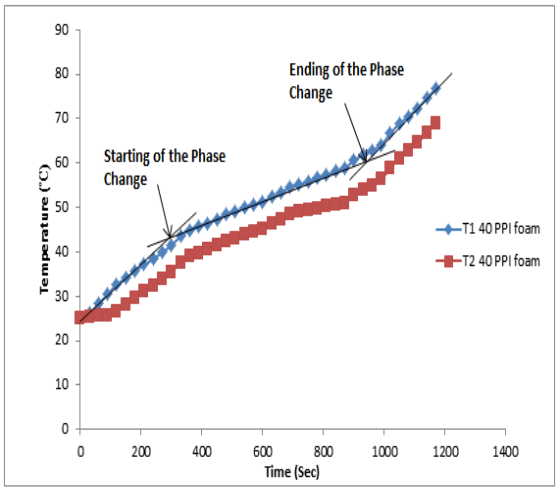

(A)

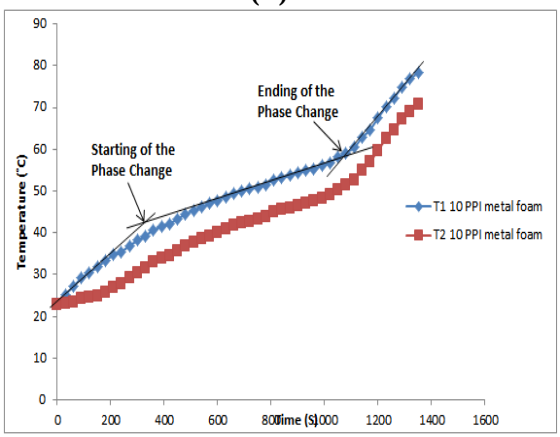

(B)

Figure 23 : Beginning and End of Melting of PCM Inserted with (10 and 40 PPI) Metal Foam

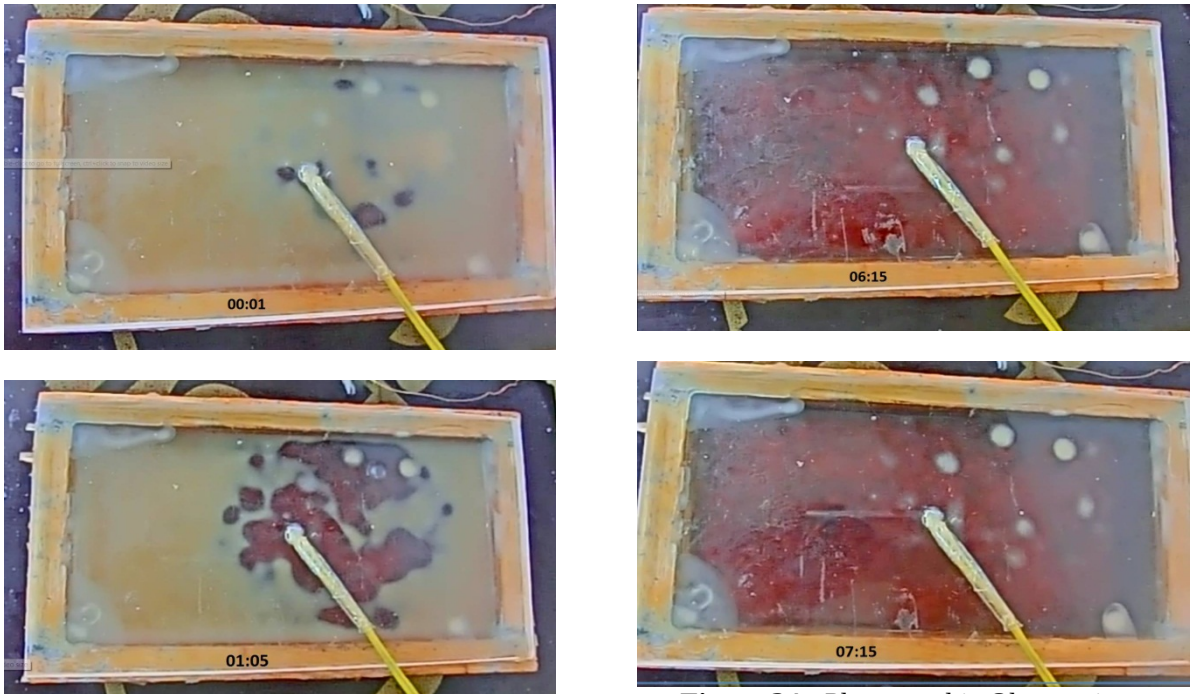

Figure 24 : Photographic Observation Showing Propagation of Melting of Wax without Metal Foam

Theoretical Results

The effective thermal conductivity was calculated theoretically by making use of equations (5) to (10) and it found to be (11.24 W/m.K). The experimental value was measured to be (8.192 W/m.K). The difference between the two values may be justified by the following factors ؛

1. The porosity of the porous medium (metal foam) is considered to be uniform but actually it varies along the length. Also the model is highly dependent on porosity. A small increase in porosity causes a large decrease in thermal conductivity .
2. Thermal resistance between the foam and copper plate is neglected in the theoretical model.

Hydrodynamic Entry Length

The hydraulic diameter of the wind tunnel test section was found from equation (18) equal to 0.2 and the boundary layer thickness found from equation (19) is found to be nearly 2 mm, the hydrodynamic entry length from equation (14) was found to be (895.9 m) at maximum flow rate of air at 100% opening. In the present work, as the length of TESS was only 200 mm, the flow was still developing and so the fluid does not feel the effect of presence of wall on the other side. Hence, the fluid motion can be considered as flow over a flat plate and the characteristic length was

taken to be the length of the copper plate L_c = 200 mm.

Verification

To verify the results obtained for the present study, a comparison was made with the results achieved by previous studies. The present results for temperature profile as a function of time for melting process for both with and without metal shown in figure (22) agrees with the results of **Zhao et al. [3]** (experimental study) shown in figure (25) which shows the result for a PCM sample with metal foam (10 PPI and 95% porosity). It is seen that the wall temperature increases steadily with a similar rate of paraffin during the whole charging process. This can be attributed to the high heat conduction through the metal foam solid structures. Figure (22) also agrees with the results of **Vadwala [4]** show in figure (26) for the temperature profile during the melting process for both with and without metal foam. It is seen that the temperature distribution when metal foam is used is more uniform than it is without the metal foam. This can be attributed to the significant increase in effective thermal conductivity due to the use of metal foam. The present results of the temperature profile as a function of time for the solidification process for both with and without metal foam shown in figure (10) agree with the results of **Vadwala [4]** shown in figure (27) for temperature results as a function of time while solidifying for both with and without metal foam at 40 L/min air mass flow rate. It is seen that with the use of metal foam it solidifies more uniformly than without metal foam and that uniformity is due to the effective thermal conductivity of foam-wax system is significantly higher than that of pure wax.

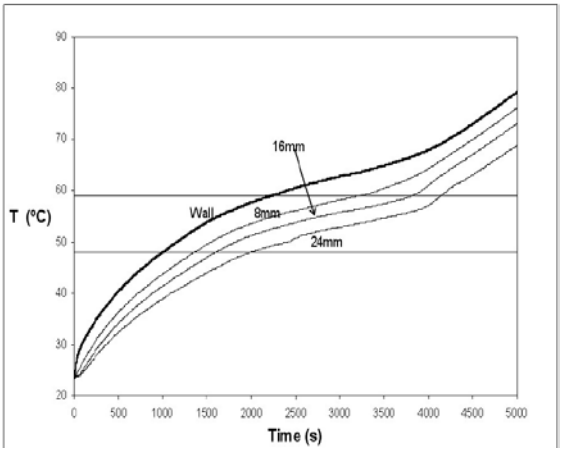

Figure (25): Temperature Variations of the Bottom Wall and the PCM at Different Locations During the Melting Process for Metal Foam Sample Zhao et al. [3]

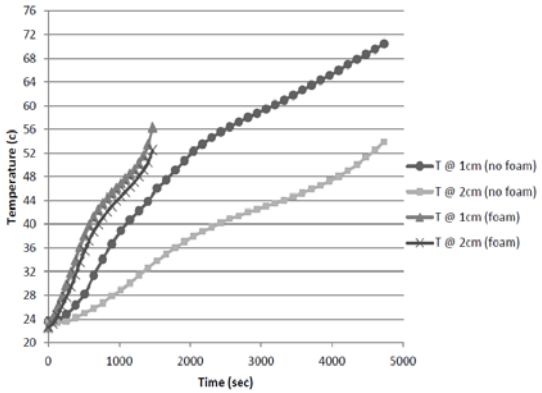

Figure 26 : Temperature Variations During the Melting Process for both with and without Metal Vadwala [4]

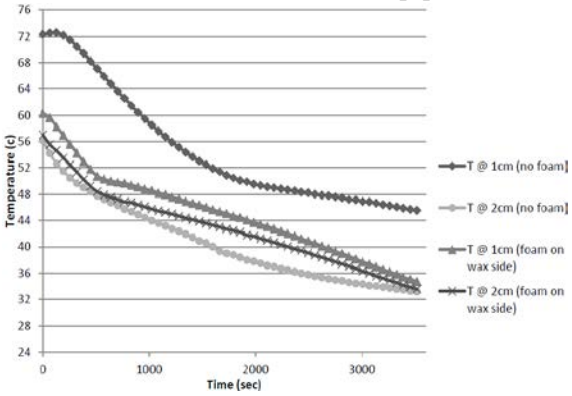

Figure 27: Experimentally Obtained Temperature Results Plotted as a Function of Time while Solidifying for Both with and without Metal Foam at 40 L/min Air Mass Flow Rate Vadwala [4]

Conclusions

The main conclusions of the present work are:

1- The ultimate goal to achieve high equivalent thermal conductivity was found in foam-wax system, with 10 PPI metal foam experimental thermal conductivity increased by (37-39) times that of pure paraffin wax RT58.

2- By using copper foam, the required time to melt a specific amount of wax was reduced by 46.7% of the required time without using metal foam for the same heat flux.

3- Two types of metal foams were used 10 PPI and 40 PPI, it concluded that the use of 40 PPI metal foam decreasing the solidification time by 25% and melting time by 8.3% from that with 10 PPI metal foam.

4- Solidification time with forced convection was lower than that with natural convection, the solidification time was reduced to 76.82% by using forced convection heat transfer at 100% air opening

Nomenclature

Latin Symbols

A	Cross-Sectional Area of Model II
A_c	Cross-Sectional Area of TESS

c_p	Specific Heat Capacity
D_h	Hydraulic Diameter
eff	Effective Value
h_a	Convective Heat Transfer Coefficient of Air
k	Thermal Conductivity
L_c	Characteristic Length
L_h	Hydrodynamic Entry Length
$\dot{m}$	Mass Flow Rate of Fluid
T_f	Temperature of the Fluid
T_i	Initial Temperature
T_m	Melting Temperature of the PCM
T_s	Surface Temperature
t	Time
u	Mean Velocity of Air

Greek Symbols

α	Thermal Diffusivity
μ	Dynamic Viscosity of Fluid
ϑ	Kinematic Viscosity
ρ	Density
δ	Boundary Layer Thickness
Δ	Difference
ε	Porosity (Percentage)

Abbreviations

PCMs	Phase Change Materials
PPI	Pore Per Inch
TESS	Thermal Energy Storage System

References

[1] Lafdi K., Mesalhy O., Shaikh S. (2007), ''Experimental study on the influence of foam porosity and pore size on the melting of phase change materials'', J. Appl. Phy.102–083549.

[2] Zhong Y., Guo Q., Li S., Shi J., and Liu L. (2010), ''Heat transfer enhancement of paraffin wax using graphite foam for thermal energy storage'', Solar Energy Materials and Solar Cells 94 P.P. 1011-1014.

[3] Zhao C.Y., Lu W., Tian Y. (2010), ''Heat transfer enhancement for thermal energy storage using metal foams embedded within phase change materials'', Solar Energy 84 (8) P.P. 1402–1412.

[4] Pathik Himanshu Vadwala (2011) '' Thermal energy storage in copper foams filled with paraffin wax'' University of Toronto.

[5] Tian Y., C.Y. Zhao, ''A numerical investigation of heat transfer in phase change materials (PCMs) embedded in porous metals'', Energy 36 (9) (2011) P.P. 5539–5546.

[6] Li W.Q., Qu Z.G., He Y.L., and Tao W.Q. (2012), ''Experimental and numerical studies on melting phase change heat transfer in open-cell metallic foams filled with paraffin'', Applied Thermal Engineering 37 P.P. 1–9.

[7] Y. Cengel (2007),"Heat and Mass Transfer" - A practical approach, 3rd ed. Mc Graw Hill, P. 901.

[8] Clamidi VV and Mahajan RL(2000), ''Forced convection in high porosity metal foams'', ASME Transactions Journal of Heat Transfer 65 P.P. 122-557.

[9] K. Boomsma (2001), "On the effective thermal conductivity of a three-dimensionally structured fluid-saturated metal foam," International Journal of Heat and Mass Transfer Vol. 44 No. 4: P.P. 827-836.

[10] Kayes W.M. and Crawford M.E. (1987), ''Convective heat and mass transfer'' Mc Graw-Hill (1993).

[11] Streeter Victor Lyle, ''Fluid mechanics'' Mc Graw-Hill.

تحسين الأداء الحراري للمواد المتغيرة الطور باستخدام الرغوات المعدنية

إحسان يحيى حسين **مروه عبد الكريم**

قسم الهندسة الميكانيكية ، كلية الهندسة، جامعة بغداد

الخلاصة:

يتضمن البحث الحالي دراسة لزيادة التوصيل الحراري وعملية الانصهار والانجماد للمواد المتغيرة الطور باستخدام رغوة معدنية. لقد تم استخدام نموذجين في التجارب العملية، النموذج الاول تم استخدامه لقياس فعالية التوصيل الحراري للمواد المتغيرة الطور المغمورة بداخلها الرغوة المعدنية، والنموذج الثاني تم استخدامه كجهاز قياس مصغر لخزن الطاقة الحرارية مع وجود الرغوة المعدنية وبدونه لدراسة عملية الانصهار و الانجماد للمادة المتغيرة الطور تحت تأثير ظروف تبريد مختلفة (حمل حراري حر و قسري). الدراسة النظرية تضمنت حل تحليلي لكلا النموذجين، الوسط شبه اللانهائي لحساب الموصلية الحرارية، و لقد تم تحليل نظام خزن الطاقة الحرارية بتضمين عدة فرضيات لتحديد معامل الحمل الحراري وكذلك العوامل التي تتحكم بالحمل الحراري القسري وعملية الانجماد للمادة المتغيرة الطور. النتائج العملية بينت ان الموصلية الحرارية للشمع مع الرغوة المعدنية ذات ال10 PPI تزداد من (37 الى 39) مرة نسبة الى الشمع النقي. تم دراسة تأثير عدة عوامل على عملية الانجماد (كثافة المسامات (10 و 40 PPI)، الرغوة المعدنية و معدل التدفق الكتلي) و ايضا تم دراسة تأثير الكثافة المسامية و أضافة الرغوة المعدنية على عملية الانصهار. النتائج العملية تمت مقارنتها مع نتائج لدراسات سابقة وكان التوافق جيد.

الكلمات الرئيسية: مواد متغيرة الطور، رغوة معدنية، مسامية، كثافة المسامات (عدد الفجوات بالانج الواحد)